

# Preliminary theoretical approach for materials elemental composition identification using X - Rays spectral transmission data

E. HERMANN<sup>a,b</sup>, O. G. DULIU<sup>c</sup>, M. IOVEA<sup>b,\*</sup>

<sup>a</sup>University of Bucharest, Faculty of Physics, Doctoral School on Physics, 405, Atomistilor str, P.O. Box – MG 11, 077125 Magurele (Ilfov), Romania

<sup>b</sup>Accent Pro 2000 ltd, 1, Nerva Traian Str., K6, 031041, Bucharest, Romania

<sup>c</sup>University of Bucharest, Faculty of Physics, Department of Structure of Matter, Earth and Atmospheric Physics and Astrophysics, 405, Atomistilor str, P.O. Box – MG- 11, 077125 Magurele (Ilfov), Romania

The paper describes a method for detection of chemical elemental composition of organic and inorganic compounds by measuring X-Ray attenuation at different energies. The method is based on the fact that the mass attenuation coefficient of a composed substance is a linear combination of the individual atoms mass attenuation weighed by the mass ratio factors. Using individual energy bin attenuation law equations, the algorithm involves an iterative method for finding best solution of linear equations system. The method was tested using attenuation data from NIST XCOM database with simulated noise. During the simulation process different values of signal to noise (SNR) ratio and different channel width of the energy bins were applied to evidence the best experimental conditions. As expected, determination of the chemical composition precision is strongly affected by the SNR of the input data. We found that reasonable results were obtained at SNR up to  $10^{-5}$  but the result precision is severely altered on higher levels of SNR. The source of the solution instability is the ill-conditioned matrix of the attenuation coefficients of the constituent elements of organic materials. However, if we reduce the range of possible solutions to a limited materials database, the algebraic method may provide substance identification with a positive false rate less than 0.7% for SNR of 0.5%. Possible practical implications of these peculiarities are discussed.

(Received January 15, 2018; accepted August 9, 2018)

**Keywords:** X-Rays, Chemical composition, Density, Material identification

## 1. Introduction

The increased frequency of terrorist attacks during last years requires the creation and implementation of new technologies to ensure civilian security.

Automatic material detection became lately a very important issue due to the new security threats and also the attempts to carry illegal substances. In the late decade, regarding the luggage scan (carry-on and checked), have been developed various automatic solutions, based on different principles: Trace analysis, Computed tomography, Dual- or multi-energy X-rays in transmission, X-rays diffraction, neutron radiography [1].

X-rays are widely used in scanning applications due to their ability to penetrate all materials and interact with all the atomic elements.

When passing through material, X- rays are attenuated following an exponential law characterized by the linear attenuation coefficient (LAC),  $\mu$ , which represents the probability of interaction between a photon and the material per unit path of length. The linear attenuation coefficient is a constant of material and depends in a complex manner on both element atomic number  $Z$  and X-ray energy  $E$ .

As it turns out, the LAC can be expressed as the product between the material density  $\rho$  and mass attenuation coefficient (MAC), whose value depended only on  $E$  and  $Z$ . For this reason, the energy dependence is the base principle for dual- and multi-energy radiography and other noninvasive control techniques [2, 3, 4, 5].

Dual energy radiography method consists of measuring the X-ray attenuation coefficient on two different energies and comparing the results with the attenuation coefficients of known materials [6, 7].

Due to the dependence of  $\mu$  on  $\rho$  and  $Z$ , it is possible, using two different energies to derive the variable couple  $(\rho, Z)$ . For compound substance an effective atomic number  $Z_{\text{eff}}$  can be defined respecting the same law as the elemental substance  $\mu_E = f(E, \rho, Z_{\text{eff}})$ .

The dual energy method involves complex practical difficulties related to the production of the dual energy beam and the separate detection. Most common techniques are: rapid kVp switching [8] dual X-ray source [9] and energy-sensitive sandwich detectors [10, 11].

The problematic of this method is related to the difficulty of establishing the  $Z_{\text{eff}}$  due to it's various interpretations [12]. Another disadvantage of dual energy technique is the fact that the pair  $(\rho, Z_{\text{eff}})$  is not always sufficient to distinguish the materials.

The development of the spectrometric detectors opens the way for multi-energy systems. The actual high speed spectroscopic photon-counting detectors [13, 14, 15] are capable to measure the energy deposited by each individual photon within a high energy resolution and at counting rate higher than 10 MHz, opening the way for multi-energy radiographic and CT techniques. At the same time, the multi-energy methods use in their advantage the continuous nature of Bremsstrahlung X-ray spectrum as generated by the Coolidge X-ray generators.

In this paper we examine a method for determination of the chemical composition of a compound substance using spectral behavior of X-ray attenuation coefficient of various elements.

Rather than using classical parameterization involving analytical expressions of the attenuation coefficient for material identification, we focus in this work on algebraic approach, based on linear dependence of the mass attenuation of a compound substance on the mass attenuation of its constituents. This methodology will be employed to examine the results concerning different organic materials whose attenuation coefficients are tabled on XCOM NIST database [16].

## 2. General concepts

The photon absorption and scattering cross section involves several processes: i. coherent scattering (Rayleigh), ii. photoelectric effect, iii. Compton (incoherent) scattering, iv. electron-positron pair and triplet production, v. photonuclear absorption, each of them characterized by cross section, *i.e.*  $\sigma_{coh}$ ,  $\sigma_{pe}$ ,  $\sigma_{incoh}$ ,  $\sigma_{pg}$  and  $\sigma_{pna}$  respectively. Consequently, the total cross section becomes [17]:

$$\sigma_{tot} = \sigma_{coh} + \sigma_{incoh} + \sigma_{pe} + \sigma_{pg} + \sigma_{pna} \quad (1)$$

As for this study we will restrain photon energies less than 1 MeV as those generated by X-ray tubes, the pair production and nuclear photoelectric absorption are absent or negligible, they will be no longer referred.

For a narrow monochromatic photon beam passing a homogeneous material, the linear attenuation coefficient (LAC) is:

$$\mu = x^{-1} \ln(I / I_0) \quad (2)$$

where  $I_0$  is the incident beam intensity,  $I$  is the emergent Intensity and  $x$  is the thickness of material.

The attenuation coefficient is related to the total cross section as:

$$\mu = \sigma_{tot} n_A \quad (3)$$

where  $n_A$  is the atomic concentration (number on atoms on the unit volume) of the material, leading to a similar relation as (1) for attenuation coefficients.

For a mixture of different elements and for an energy  $E$  of the photons, MAC is the weighted average of individual MAC [17]:

$$\frac{\mu(E)}{\rho} = \sum_i w_i \frac{\mu_i(E)}{\rho_i} \quad (4)$$

where  $w_i$  are the weight fractions of the element  $i$ .

The target of this paper is to investigate the possibility of material identification by measuring the attenuation coefficient at different energies and comparing the result with the pre-calculated data from a database. To accomplish this task, we have used the National Institute for Standards and Technology (NIST) X-Ray mass attenuation data.

## 3. Detecting density and chemical formula of unknown substances

The spectrum produced by a typical X-ray tube represents a superposition of a continuous component due to the electron Bremsstrahlung and of the characteristic X-ray of the anode material [18] (Fig. 1). In these conditions, for a polychromatic X-rays spectrum, the exponential attenuation law becomes:

$$I(E) = I_0(E) e^{-\mu(E)x} \quad (5)$$

where  $E$  varies between  $E_{min}$  and the  $E_{max}$ .

Measuring the photon intensity on individual energy intervals and determining the MAC for each interval, may provide the information for finding the chemical components of the analyzed substance, as MAC dependence on energy differs from material to material.

Assuming the material has  $n$  possible constituent elements and the attenuation coefficients are measured for  $m$  energy channels, we can write the equation (4) individually for each channel. Considering that MAC is well known for each chemical element on a given energy, equations (4) will assembly a system of linear equations with  $n$  unknown variables (corresponding to  $w_i$  terms) and  $m$  equations. In this paper we will not deal with underdetermined system of equations, therefore we will consider that the MAC can be determined for a large enough number  $m$  of energies *i.e.*  $m \geq n$ .

$$\frac{\mu(E_j)}{\rho} = \sum_{i=1}^n w_i \frac{\mu_i(E_j)}{\rho_i} \quad (6)$$

$$j = 1, 2, 3, \dots, m$$

Consequently, we have to solve the system (6) consisting of  $m$  equations with the obvious constrain:

$$\sum_{i=1}^n w_i = 1 \quad (7)$$

Next, we delimitate the quantities that can be measured by X-ray transmission, therefore we multiply the eq. (6) with the material density  $\rho$  and obtain the new system of equations:

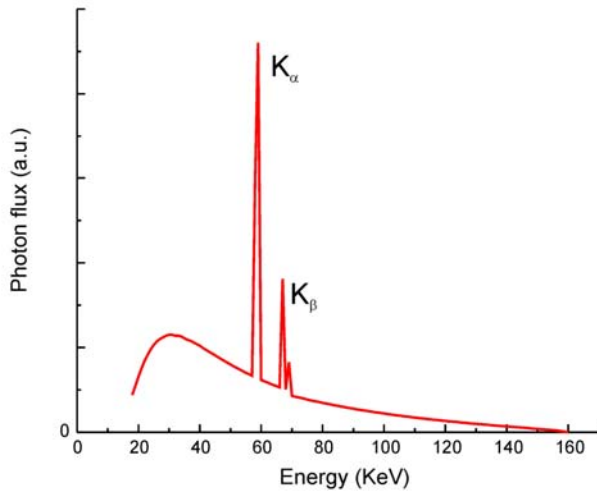


Fig. 1. The energy spectrum of the 160 kV, W-anode X-ray generator used in simulation

$$\mu(E) = \sum_{i=1}^m c_i \frac{\mu_i(E)}{\rho_i} \quad (8)$$

where new unknown variables are the quantities  $c_i = w_i \rho$  representing the constituent density ratio.

According to: (7) the sum of density ratios becomes:

$$\sum_i c_i = \rho \quad (9)$$

Finally, the solution of the equations (8) will lead to  $c_i$  values whose sum represents, according to eq. (9), the unknown substance density  $\rho$  and can calculate, according to  $c_i$  expression, the corresponding constituents mass ratios  $w_i$ .

The system (8) is a system of linear equations of type  $\mathbf{Ax}=\mathbf{B}$  where the elements of matrix  $\mathbf{A}$  and the vector  $\mathbf{B}$  are determined with a limited precision.

Therefore, an algorithm that will provide approximate solutions, stable to uncertainties  $\delta\mathbf{B}$  in measuring  $\mathbf{B}$ , should be employed. Iterative method based on the least-squares constraints and singular value decomposition (SVD) - based methods with different regularizations were compared.

Table 1. Condition number of mass attenuation coefficients matrix for different energy bins, for the tested elements

Energy range	Chanel width	C= $\sigma_{\text{Max}}/\sigma_{\text{Min}}$
18-160 KeV	$\Delta E=1\text{KeV}$	$\sim 10^5$
18-160 KeV	$\Delta E=2\text{KeV}$	$\sim 10^5$
18-160 KeV	$\Delta E=4\text{KeV}$	$\sim 10^6$
18-160 KeV	$\Delta E=8\text{KeV}$	$\sim 10^6$

#### 4. Materials and methods

We have check this procedure by considering a set of 13 low density and low atomic numbers substances, i.e. water, polyethylene, polystyrene, polymethyl methacrylate, polyethylene terephthalate, teflon, polyvinylchloride, ethanol, calcium sulfate, ammonium nitrate, nitroglycerin, trinitrotoluene and cyclotrimethylene trinitramine (RDX).

We have considered an X-rays generator with a wolfram anode and a maximum anodic potential of 160 kV whose spectrum, simulated by means of SpekCalc program [19], is reproduced in Fig. 1.

For the candidate constituent elements, we considered 19 common elements from database, namely the elements with the atomic number  $Z$  equal to 1,6,7,8,9,11,12,13,14,15,16,17,19,20,26,27,28,29, and 30.

Numerically we use different approaches for minimizing the norm:

$$\left\| \mu(E) - \sum_i c_i \frac{\mu_i(E)}{\rho_i} \right\| \quad (10)$$

Nonnegative least square methods will minimize the norm (10) with the constraints  $c_i \geq 0$ .

Single value decomposition (SVD) offers alternative ways to solve the equation (8).

The matrix of mass attenuation coefficients  $\mathbf{A}=[\mu_i(\mathbf{E})/\rho_i]$  which is of a  $m \times n$  ( $m$  is number of bins and  $n$  is number of elements) type, can be decomposed uniquely as:

$$\mathbf{A} = \mathbf{U} \mathbf{S} \mathbf{V} \quad (11)$$

where  $\mathbf{U}$  is a  $m \times m$  orthogonal matrix,  $\mathbf{V}$  is an orthogonal  $n \times n$  matrix and  $\mathbf{S}$  is a  $m \times n$  diagonal matrix.

SVD provides a way of calculating the inverse of matrix  $\mathbf{A}$ :

$$\mathbf{A}^{-1} = \mathbf{V} [\text{diag}(\sigma_1^{-1} \sigma_2^{-1} \sigma_3^{-1} \dots \sigma_n^{-1})] \mathbf{U}^T \quad (12)$$

where  $\sigma_i$  are the elements of matrix  $\mathbf{S}$ .

The solution of the system of a linear equations system  $\mathbf{Ax}=\mathbf{B}$  is:

$$x = V \left[ \text{diag}(\sigma_1^{-1} \sigma_2^{-1} \sigma_3^{-1} \dots \sigma_n^{-1}) \right] (U^T b) \quad (13)$$

If at least one of the elements  $\sigma_i$  is zero, then the matrix  $A$  is singular and if the minimum  $\min(\sigma_i)$  is too small the matrix  $A$  is ill-conditioned. In both cases the expression (13) for the equation system becomes problematic due to division by zero. For ill conditioned problems it is relevant to establish a numeric evaluation of the singularity, meaning how singular is the matrix  $A$ .

The condition number  $C$  of matrix  $A$  is defined as the ration of its largest singular value to its smallest singular value:

$$C = \frac{\max(\sigma_i)}{\min(\sigma_i)} \quad (14)$$

As is shown in *Table 1* the system of equations 8 is a ill conditioned problem and we applied regularization recipes for solving it.

The following regularization methods were tested:

- Tikhonov regularization [23] minimizing the quantity  $\|Ax-B\|^2 + \lambda\|x-x_0\|^2$
- Least square with quadratic constraint [24] minimizing the norm  $\|Ax-B\|$  subject to  $\|x\| < \theta$
- Truncate SVD [25],
- Maximum Entropy [26] minimizing the quantity  $\|Ax-B\|^2 - \lambda^2 \cdot \text{Entropy}$

## 5. Results and discussion

The method was tested for different composed substances, using as input the XCOM data [16]. To get the best sampling ratio, we have performed several tests by using 1, 2, 4 and 8 keV channel width, *i.e.* compatible with the energy resolution of the actual CdTe and CdZnTe detectors [20, 21]. The MAC values per channel were calculated by data integration within the channel width. At the same time, to be closer to experimental conditions, in all cases, we have superimposed a random noise as a percent of the transmitted spectrum value, so that the Signal to Noise Ratio (SNR) varied between 100000 and 100.

To quantify the uncertainty in determining both chemical composition and density, we have the variance of the mass concentrations of the composing element reported to the content of the same material as well the variance of density as provided by XCOM (Hubbell and Seltzer, 2016), according to the equation:

$$\text{var} = \sqrt{\sum_i \left( \frac{c_{\text{exp},i} - c_{0,i}}{c_{0,i}} \right)^2} \cdot 100 \% \quad (15)$$

where  $c_{\text{exp},i}$  and  $c_{0,i}$  represent the mass fraction of the element  $i$  calculated and provided by the XCOM data respectively.

The same equation, but restrained only to one term was used in the case of density.

The most important results of our simulations are reproduced in the Table 1 A (Annex 1) and illustrated as contour maps in Fig. 2, while a complete list of simulated data can be found in the supplementary material.

As a rule, for all materials, the variance decreases with the SNR as well as with the bin width, so from this point of view the 8 keV seems a better choice. But even in this case, the SNR ratio plays the major role, as, by reducing it ten times, the average uncertainty increases about 25 times in the case of chemical composition and about 20 times in the case of density. At the same time, the uncertainty regarding chemical composition remained about one to three order of magnitude greater the those corresponding to the density one (see Fig. 3 for exemplification).

Moreover, for all materials, the uncertainty in determining the chemical composition inversely correlates with the SNR, so greater the SNR, the lower uncertainty in determining both chemical composition and density. In this regard, some illustrative examples are reproduced in Fig. 4.

In all our simulations, we have considered that the SNR is mainly due to the statistic fluctuation, which are better described by the Poisson law of distribution and are equal to square root of the count number. Consequently, for SNR between 100 and 1000 and 8 keV bin, for which the uncertainties in estimating the chemical composition have reasonable values, it would be necessary counting rates greater than 10 kHz, values which the modern CdZnT and the associated electronic could easily provide.

An important aspect is the analysis of solution stability for which we recall the SVD formalism. The condition number  $C$ , presented in Table 1 estimates the degree of singularity and it is related to precision obtained in solving the system of linear equations (11).

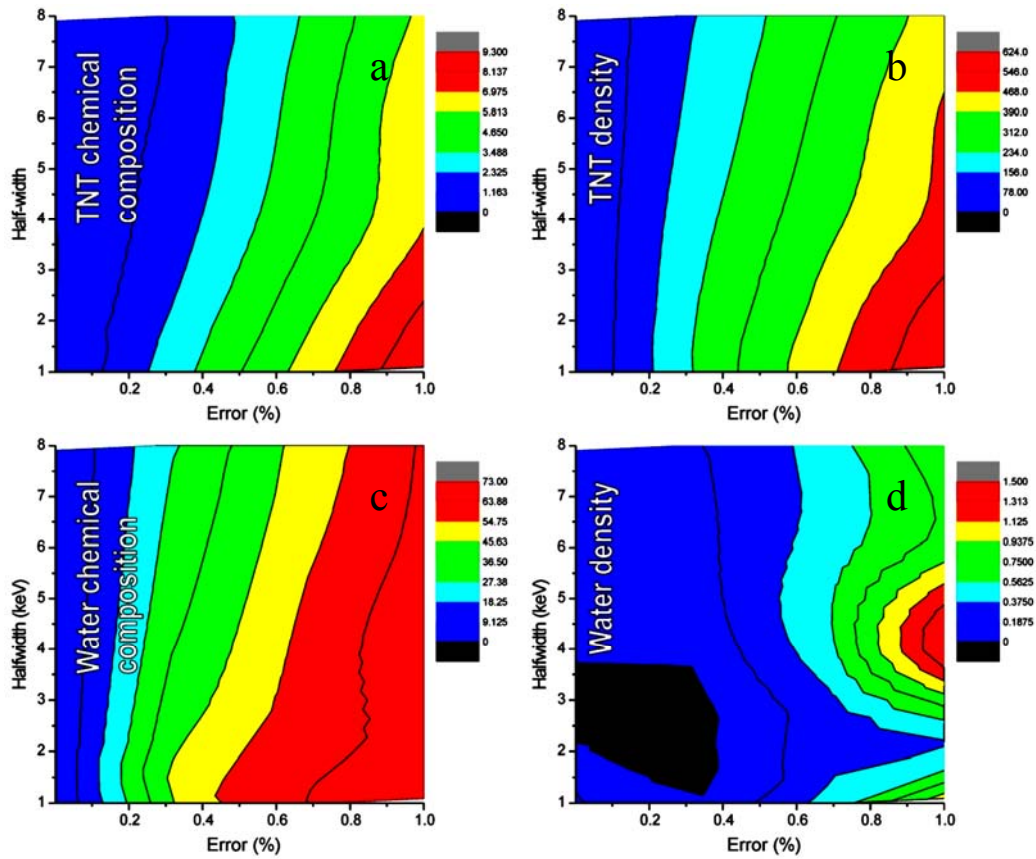


Fig. 2. Four surface plots showing the dependence of the chemical composition (a and c) and density (b and d) uncertainties on SNR and bin width in the case of TNT (a and b) and water (c and d)

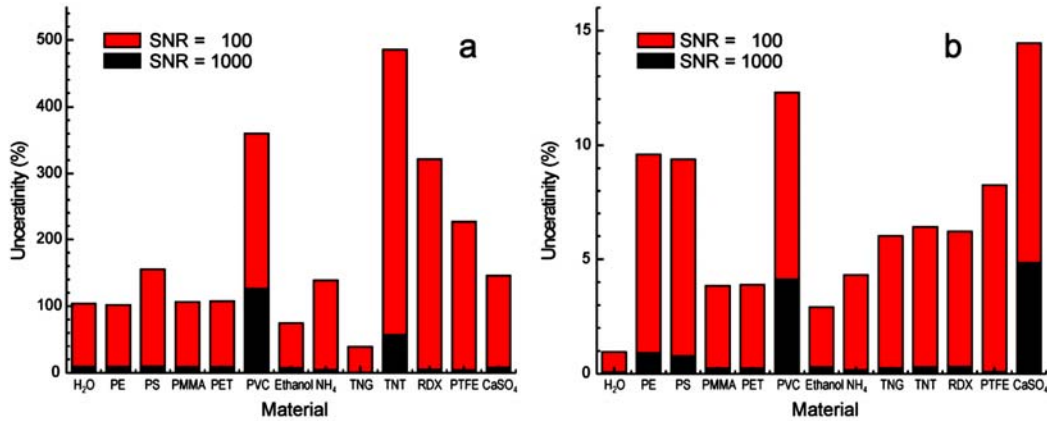


Fig. 3. The uncertainties in determining chemical structure (a) and density (b) for all materials and for two different values of the SNR, i.e. 100 and 1000. High uncertainties correspond to SNR lower value

If the vector  $\mathbf{B}$  is perturbed with  $\delta\mathbf{B}$ , than the variation of the solution  $\mathbf{x}$  obtained by direct inversion of  $\mathbf{A}$  will be related to variation of  $\mathbf{B}$  according to [27]:

$$\frac{\delta\mathbf{x}}{\mathbf{x}} \leq C \frac{\delta\mathbf{B}}{\mathbf{B}} \quad (15)$$

Relation (15) states that in the worst case, the relative uncertainty of the equation system solution is amplified by  $C$  factor.

For our problem, in equation (8) the elements of  $\mathbf{B}$  are the measured attenuation coefficients at different energies. The analyzed data suggest that in order to determine a stable solution using direct solving methods for equation (8) the source attenuation coefficient should be determined with an uncertainty lower than  $10^{-6}$ .

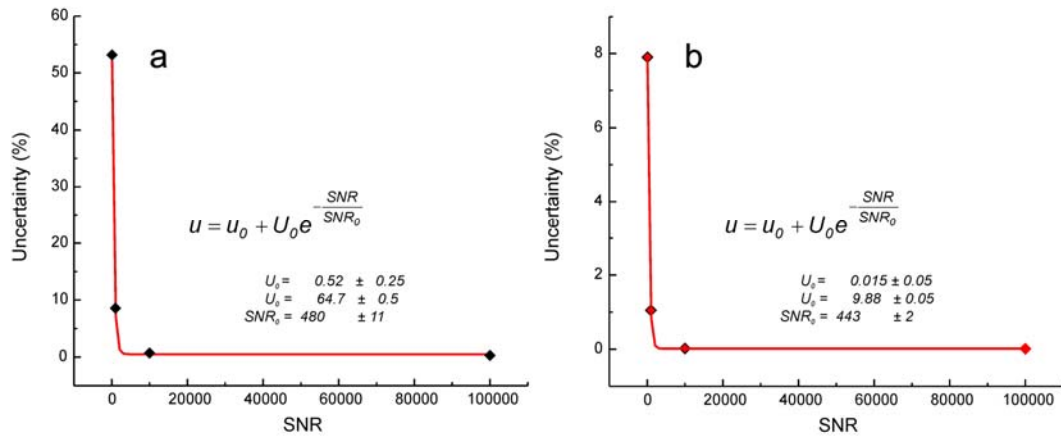


Fig. 4. Two bi-plots illustrating the exponential decay type dependence of both chemical composition and density uncertainties on the SNR in the case of TNG.

Although the SNR of  $10^6$  implies a considerable flux of photons/bin ( $\sim 10^{12}$ ) we obtained good results on SNR ratio of  $10^4$ .

The method was also tested against a predefined material database consisting of the 30 common substances

organic and inorganic with low density and low atomic number constituents presented in Table 2. In this case we assumed that the solution of the system (8) should be one of the substances from the database.

Table 2. Database of 30 substances with low density and low atomic number constituents

Substance	Nature	Density (g/cm <sup>3</sup> )	Substance	Nature	Density (g/cm <sup>3</sup> )
Graphite	Inorganic	1.80	HMTD	Explosive	0.90
H <sub>2</sub> O	Water	1.00	Uric acid	Precursor	1.90
H <sub>2</sub> O <sub>2</sub>	Precursor	1.50	TNT	Explosive	1.70
Polyethylene	Polymer	0.93	Ammonium picrate (Dunnite)	Explosive	1.70
PA12	Polymer	1.02	Nitromethane	Explosive	1.10
PMMA	Polymer	1.18	Nitroglycerine	Explosive	1.60
PET	Polymer	1.38	Cyclonite (RDX)	Explosive	1.82
Delrin	Polymer	1.40	HMX (Octogen)	Explosive	1.90
PVC	Polymer	1.41	Nitrocellulose	Explosive	1.30
Sorbitol	Sugar	1.50	PETN (Penthrite)	Explosive	1.80
Sugar (Saccharose)	Sugar	1.60	Ammonium nitrate	Explosive	1.80
Fructose	Sugar	1.50	PVDF	Organic	1.78
Polystyrene	Polymer	0.96	PTFE	Teflon	2.25
Acetone peroxide: TATP (dimer)	Explosive	0.70	CaSO <sub>4</sub>	Inorganic	2.96
Acetone peroxide: TATP (trimer)	Explosive	1.22			

Taking the advantage of the good precision on density determination, the solutions were filtered sequentially, first by applying density uncertainty threshold criteria and secondly using the chemical composition uncertainty criteria.

The false positive rates at different noise levels, for different bin widths are shown in Fig. 5. With this constrains the identification algorithm yields to precise result on lower levels of SNR.

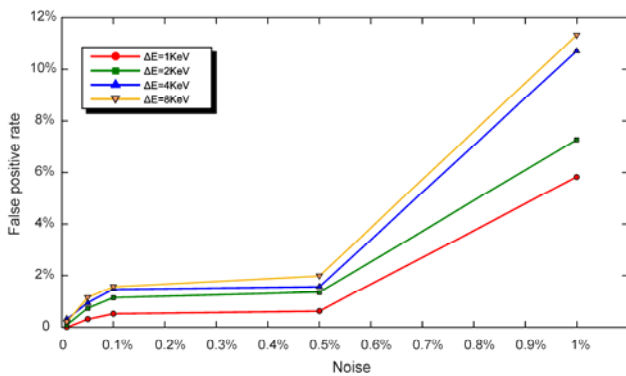


Fig. 5. False positive rates of material identification at different noise levels, for different bin widths

This method produces false positives with a rate less than 2% for a SNR of 0.5%, achievable when  $4 \times 10^4$  photons/bin are detected.

## 6. Conclusion

In recent years, due to the increased threats to passenger's security, the automatic detection of dangerous substances has become an important objective.

The results of our study show clearly that X-ray radiographic investigation of the materials on multi-energy can provide a viable method for finding the precise chemical composition. The inversion of mass ratio coefficients matrix method was tested on theoretical case, using calculated values for the attenuation. The tests included simulations on organic compounds with low effective atomic number, including some explosive materials.

Providing accurate measurements of attenuation coefficient on different energies, with relative error of less than  $10^{-5}$ , one can clearly obtain the tested substance density and chemical composition without any previous information or assumptions regarding the scanned material.

The identification of materials is dramatically improved when the solution range is limited to a material database, providing substance identification with a positive false rate less than 0.7% for data measured with a relative incertitude of  $0.5 \times 10^{-2}$ .

## References

[1] K. Wells, D. A. B. Bradley, *Applied Radiation and Isotopes* **70**, 1729 (2012).  
 [2] S. M. Midgley, *Physics in Medicine and Biology* **50**, 4139 (2005).  
 [3] C. H. McCollough, S. Leng, L. Yu, et al., *Radiology* **276**, 637 (2015).  
 [4] A. Saversky, D-C. Dinca, J. M. Rommel, *Physics Procedia* **66**, 232 (2015).

[5] J. M. S. Wait, D. Cody, A. K. Jones, et al., *American Journal of Roentgenology* **204**, 1234 (2015).  
 [6] R. E. Alvarez, A. Macovski, *Physics in Medicine and Biology* **21**,733 (1976).  
 [7] A. Macovski, R. E. Alvarez, J. L. Chan, J. P. Stonestrom, L. M. Zatz, *Computers in Biology and Medicine* **6**, 325 (1976).  
 [8] W. A. Kalender, W. H. Perman, J. R. Vetter, E. Klotz, *Medical Physics* **13**, 334 (1986).  
 [9] T. G. Flohr, C. H. McCollough, Bruder, et al., *Eur Radiol.* **16**, 256 (2006).  
 [10] V. Rebuffel, J. M. Dinten, *Insight - Non-Destructive Testing and Condition Monitoring* **49**(10), 589 (2007).  
 [11] D. T. Boll, E. M. Merkle, E. K. Paulson, et al., *Radiology* **247**, 687 (2008).  
 [12] Ph. Duvauchelle, G. Peix, D. Babot, *Nuclear Instruments and Methods in Physics Research B* **155**, 221 (1999).  
 [13] D. Kang, D. Lee, M. Cho, et al., *Proc. 2015 IEEE International Conference on Consumer Electronics (ICCE)*, Las Vegas, NV **2015**, 614 (2015) -615.  
 [14] B. Dierickx, Q. Yao, N. Witvrouwen, et al., *Sensors* **16**, 764 (2016).  
 [15] T. Hugh, H. T. Philipp, M. W. Tate, P. Purohit, et al., *Journal of Synchrotron Radiation* **23**, 395 (2016).  
 [16] J. H. Hubbell, S. M. Seltzer, *Tables of X-Ray Mass Attenuation Coefficients and Mass Energy-Absorption Coefficients (version 1.4)* [Online] Available: <http://physics.nist.gov/xaamdi>, National Institute of Standards and Technology, Gaithersburg, MD (2004).  
 [17] G. E. Hine, *Nucleonics* **10**, 9 (1952).  
 [18] N. Broll, P. de Chateaubourg, *JCPDS-International Centre for Diffraction Data* **1999**, 393 (1999)  
 [19] G. G. Poludniowski, P. M. Evans, *Medical Physics*,**34**(6), 2164-74 (2007).  
 [20] T. Schlesinger, J. Toney, H. Yoon, et al., *Materials Science and Engineering: R: Reports* **32**, 103 (2001).  
 [21] Q. Zhang, C. Zhang, Y. Lu, et al., *Sensors* **13**, 2447 (2013).  
 [22] E. Trucco, A. Verri, *Introductory Techniques for 3D Computer Vision*, Appendix A.6, Prentice Hall, ISBN 0-13-261108-2 (1998).  
 [23] A. N. Tikhonov, V. Y. Arsenin, *Solutions of Ill-Posed Problems*, Winston & Sons, Washington, D.C., 1977.  
 [24] A. Björck, *Numerical Methods in Matrix Computations*, p. 348-356, Springer 2015.  
 [25] P. C. Christian Hansen, *The truncated SVD as a method for regularization*, Numerical Analysis Project Computer Science Department, Stanford University Stanford, 1986.  
 [26] R. Fletcher, *Practical Methods of Optimization*. Vol. 1, *Unconstrained Optimization*, Wiley, Chichester, 1980.  
 [27] G. Arfken, *Ill-Conditioned Systems. Mathematical Methods for Physicists*, 3rd ed. Academic Press, Orlando, FL, pp. 233 (1985).

\*Corresponding author: office@accent.ro

**Annex 1**

*Table 1A Numerical values of uncertainty in determining the chemical composition (Chem uncert) as well in determining of density ( $\rho$  uncert) as a function of signal to noise ratio (SNR) and bin width for each considered material.*

Material	SNR	Bin width (keV)	Chem Uncer (%)	$\rho$ uncert (%)	Material	SNR	Bin width (keV)	Chem uncert (%)
<b>Water</b>	10000	1	2.0	0.7	<b>NH4</b>	10000	1.3	0.0
	10000	2	1.7	0.1		10000	0.6	0.0
	10000	4	1.2	0.1		10000	0.6	0.0
	10000	6	0.9	0.0		10000	0.4	0.0
	10000	8	0.7	0.1		10000	0.8	0.0
	1000	1	23.0	0.2		1000	19.0	0.5
	1000	2	18.0	0.0		1000	11.5	0.3
	1000	4	13.0	0.0		1000	6.7	0.1
	1000	6	11.0	0.0		1000	5.3	0.0
	1000	8	9.0	0.1		1000	4.3	0.2
	100	1	73.0	1.1		100	183.4	5.7
	100	2	67.0	0.3		100	188.3	5.6
	100	4	71.0	1.5		100	164.3	4.9
	100	6	67.0	0.8		100	143.8	4.2
	100	8	65.0	0.9		100	134.9	4.1
<b>PE</b>					<b>TNG</b>			
	10000	1	1.8	0.2		10000	0.7	0.0
	10000	2	1.2	0.1		10000	0.8	0.0
	10000	4	1.0	0.1		10000	0.6	0.1
	10000	6	0.8	0.1		10000	1.3	0.1
	10000	8	0.9	0.1		10000	1.2	0.1
	1000	1	19.0	2.0		1000	8.6	1.1
	1000	2	12.0	1.4		1000	7.9	0.8
	1000	4	10.0	1.1		1000	7.6	0.5
	1000	6	7.0	0.9		1000	6.6	0.3
	1000	8	9.0	0.9		1000	0.6	0.2
	100	1	172.0	15.0		100	53.1	7.9
	100	2	135.0	12.0		100	45.9	6.8
	100	4	120.0	11.0		100	40.2	6.0
	100	6	99.0	9.1		100	37.3	5.5
100	8	93.0	8.7	100	38.6	5.8		
<b>PS</b>					<b>TNT</b>			
	10000	1	4.5	0		10000	6.9	0.0
	10000	2	3.6	0		10000	7.8	0.0
	10000	4	3.8	0		10000	11.0	0.0
	10000	6	3.7	0		10000	11.0	0.0
	10000	8	3.8	0		10000	15.2	0.0
	1000	1	30.1	2		1000	83.4	1.0
	1000	2	17.0	1		1000	79.9	0.6
	1000	4	14.0	1		1000	76.3	0.4
	1000	6	10.4	1		1000	60.5	0.2
	1000	8	9.5	1		1000	56.8	0.3
	100	1	294.0	15		100	622.5	9.3
	100	2	232.0	13		100	591.6	8.5
	100	4	160.0	9		100	492.5	6.9
	100	6	188.0	11		100	477.8	6.8
100	8	146.0	9	100	429.0	6.1		
<b>PMMA</b>					<b>RDX</b>			
	10000	1	33.0	0.2		10000	4.7	0.0
	10000	2	3.3	0.0		10000	5.8	0.0
	10000	4	3.4	0.0		10000	6.4	0.0
	10000	6	1.7	0.0		10000	7.8	0.0
	10000	8	2.5	0.0		10000	8.2	0.0
	1000	1	44.0	0.0		1000	6.9	1.1

Material	SNR	Bin width (keV)	Chem Uncer (%)	$\rho$ uncert (%)	Material	SNR	Bin width (keV)	Chem uncer (%)
	1000	2	17.0	0.2		1000	5.2	0.6
	1000	4	19.0	0.2		1000	5.1	0.3
	1000	6	13.0	0.2		1000	5.0	0.4
	1000	8	8.6	0.2		1000	4.7	0.3
	100	1	183.0	7.3		100	448.5	8.4
	100	2	162.0	6.7		100	410.9	7.4
	100	4	140.0	4.9		100	334.8	6.0
	100	6	120.0	4.4		100	323.3	5.9
	100	8	98.0	3.6		100	317.31	5.8831
<b>PET</b>					<b>PTFE</b>			
	10000	1	3.4	0.0		10000	11.1	0.3
	10000	2	2.0	0.1		10000	11.1	0.2
	10000	4	2.5	0.1		10000	8.4	0.2
	10000	6	2.5	0.1		10000	5.4	0.1
	10000	8	2.8	0.1		10000	3.7	0.1
	1000	1	0.0	0.0		1000	61.1	2.6
	1000	2	17.4	0.2		1000	63.0	2.2
	1000	4	19.7	0.2		1000	66.2	1.8
	1000	6	12.9	0.1		1000	56.8	1.5
	1000	8	8.6	0.2		1000	52.8	1.3
	100	1	183.8	7.3		100	244.8	10.7
	100	2	162.5	6.7		100	221.5	9.9
	100	4	140.3	4.9		100	226.2	9.0
	100	6	119.9	0.4		100	216.8	8.2
	100	8	98.8	3.6		100	223.5	8.2
<b>PVC</b>					<b>CaSO<sub>4</sub></b>			
	10000	1	35.6	1.4		10000	1.2	2.2
	10000	2	26.8	0.1		10000	1.5	1.0
	10000	4	19.9	0.7		10000	1.2	0.7
	10000	6	12.6	0.5		10000	8.2	0.5
	10000	8	14.5	0.6		10000	8.5	0.5
	1000	1	167.2	5.4		1000	7.6	6.6
	1000	2	142.9	4.6		1000	8.9	5.9
	1000	4	139.8	4.8		1000	4.4	5.4
	1000	6	135.6	4.5		1000	7.9	4.8
	1000	8	125.8	4.1		1000	7.8	4.9
	100	1	244.8	10.7		100	120.0	12.9
	100	2	221.5	9.9		100	122.3	11.4
	100	4	226.2	9.0		100	124.6	10.3
	100	6	216.7	8.2		100	133.2	9.8
	100	8	234.4	8.2		100	138.2	9.6
<b>Ethanol</b>								
	10000	1	0.9	0.05				
	10000	2	0.8	0.04				
	10000	4	0.5	0.04				
	10000	6	9.6	0.04				
	10000	8	7.0	0.05				
	1000	1	16.2	0.06				
	1000	2	14.0	0.14				
	1000	4	13.3	0.16				
	1000	6	9.6	0.15				
	1000	8	7.0	0.30				
	100	1	112.7	4.80				
	100	2	97.4	3.80				
	100	4	96.9	3.06				
	100	6	84.6	2.90				
	100	8	67.5	2.62				